stellarator news

Published by Fusion Energy Division, Oak Ridge National Laboratory
Building 9201-2; P.O. Box 2009; Oak Ridge, TN 37831-8071, USA

Editor: James A. Rome Issue #12 November, 1990

Eighth International Workshop on Stellarators

The Eighth International Workshop on Stellarators will be held in Kharkov, U.S.S.R., May 27–31, 1991. This is the week before the 18th European Conference on Controlled Fusion and Plasma Physics in Berlin, FRG. The five-day workshop, organized by the IAEA, will have both the usual formal talks and discussion sessions focusing on selected key issues in stellarator research.

The proceedings of the last of these biennial workshops, held in Oak Ridge, TN, USA, in 1989, has been published by the IAEA as IAEA-TECDOC-558, *Stellarator Physics.* A limited number of copies are available from J. F. Lyon at Oak Ridge National Laboratory or through the IAEA.

Previous International Stellarator Workshops were held in Kyoto, Japan (1986), Lake Tegernsee, FRG (1984 and 1980), Cape May, USA (1982), and Moscow, USSR (1981). For more information, please contact J. F. Lyon (ORNL) or E. Oktay (DOE-OFE) in the USA; G. Grieger (IPP Garching) in Europe; A. Iiyoshi (NIFS, Nagoya) in Japan; or L. M. Kovrizhnykh (IGP, Moscow) or O. S. Pavlichenko (KPTI, Kharkov) in the USSR.

Sheffield and Painter Recieve ANS Awards

John Sheffield, Director of ORNL's Fusion Energy Division, received the 1990 Outstanding Achievement Award of the American Nuclear Society in recognition of his exemplary achievements in professional excellence and leadership in the area of fusion science and engineering.

Scott Painter, a doctoral candidate at the University of Tennessee, received the ANS 1990 Fusion Engineering Division Student Award for a *Fusion Technology* paper, "Alpha-Particle Losses in Compact Torsatron Reactors." This paper was based on research performed at Oak Ridge National Laboratory and formed part of Mr. Painter's PhD dissertation, "Performance Analysis and Parametric Optimization Study of Torsatron Fusion Reactors." Scott's advisors were Jim Lyon at Oak Ridge and Paul Stevens at UT. After graduating in December 1990, Mr. Painter will join the Plasma Research Laboratory at the Australian National University.

Both awards were presented at the Ninth Topical Meeting on the Technology of Fusion Energy in Chicago during October.

Meeting Reports

IEA Stellarator Workshop on Future Large Devices October 8–9, 1990 Oak Ridge, TN, USA

This was the third workshop held on this topic; previous workshops were held at Kyoto, Japan (July 1988), and at Toki and Nagoya, Japan (December 1989), as reported in the March 1990 issue of *Stellarator News.* Approximately 25 participants from the USA, Japan, the FRG, Spain, Australia, and Switzerland presented 17 papers on the physics and engineering optimization of the large next-generation stellarators, Wendelstein VII-X (W VII-X) and the Large Helical Device (LHD), stellarator reactor studies, and relevant research on present experiments (W VII-AS, CHS, ATF, and Heliotron-E).

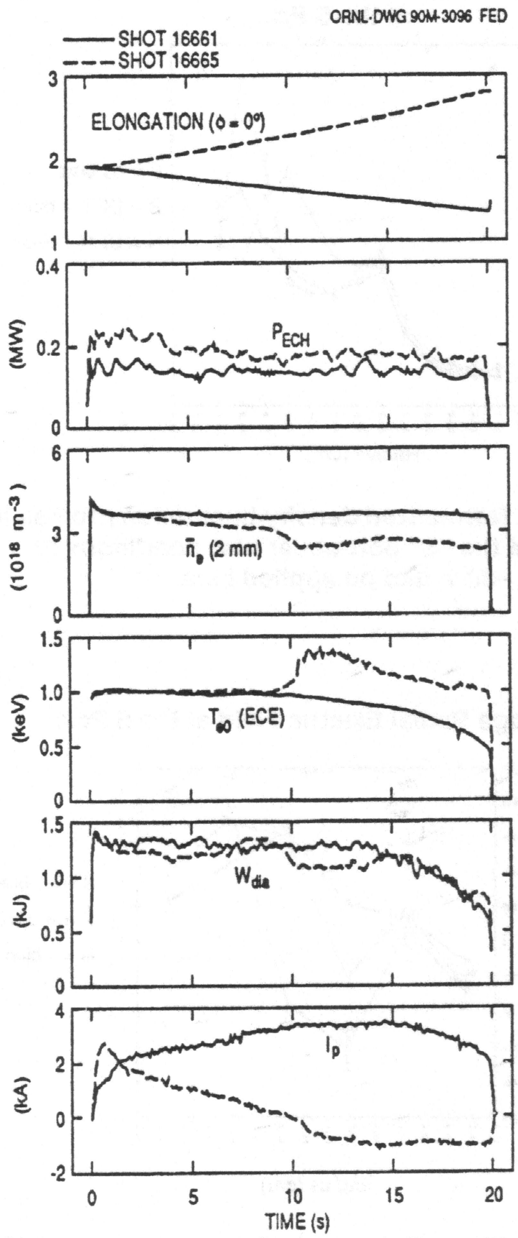

Fig. 1. Time histories of plasma parameters in two 20-s ECH discharges in which configuration (elongation) was dynamically changed at B_0 = 0.95 T and R_0 = 2.08 m.

two fixed pressure profiles (at two extreme cases that bracket the experimental profiles in stationary discharges). This result shows that the basic dependence on the quadrupole moment is through the geometrical factor G (or neoclassical viscosity due to the magnetic field structure), rather than through changing plasma parameters, and confirms the neoclassical description of the current observed in ECH discharges in ATF.

The ATF experiment was shut down at the end of September for three months to upgrade a 13.8-kV transformer vault.

Masanori Murakami for the ATF Group
Oak Ridge National Laboratory
P. O. Box 2009, MS 8072
Oak Ridge, TN 37831-8072, USA

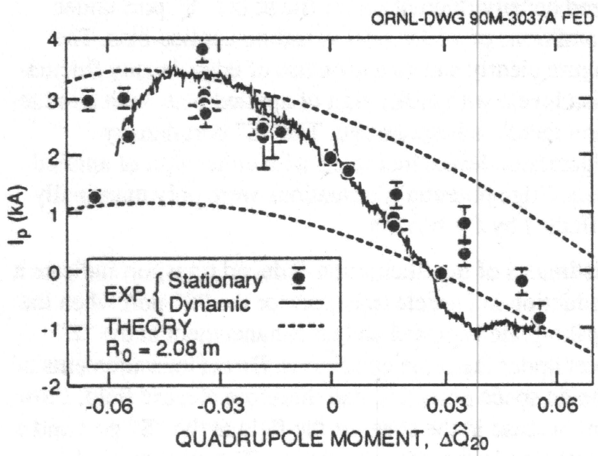

Fig. 2. Current as a function of quadrupole moment. Experimental values are from stationary discharges (closed points) and dynamic configuration scans during long ECH discharges (continuous curve). Theoretical estimates (dashed curves) for neoclassical bootstrap current are based on two fixed pressure profiles.

News from CHS

ECH experiments with focusing mirror launcher

The launcher for 53-GHz microwaves has been replaced with a new design which is able to focus the beam. The motivation for installation of a focusing launcher is first to increase the heating efficiency of the microwaves by concentrating the heating power at the center of plasma and second to get a more reliable picture of the power deposition profile, which is needed to perform local transport analysis. The effects of focusing have been confirmed by some experimental results. In a series of shots where the magnetic field strength was varied, stronger heating was observed when the focusing spot was on the ECH resonance layer, for cases when the resonance was at the plasma center or shifted from the center.

However, the overall heating efficiency has not been increased so much. This is partly because the one-pass absorption is not sufficient with present plasma parameters. Another reason is that part of the microwave power is focused but the rest of power is still launched without focusing because of the geometrical limitation of the focusing mirror.

Toroidal rotation measurement with TVCXS

Profiles of toroidal rotation for tangential neutral beam injection (both co- and counter-injection) were obtained using the TV charge-exchange spectroscopy (TVCXS) with 38 channels aligned vertically. The toroidal rotation speed depends on the setting of magnetic axis position, and the maximum value was 30–40 km/s at the plasma center for configurations with a vacuum magnetic axis position (R_{ax}) at 90–92 cm. The real magnetic axis position is shifted by 3–4 cm due to the pressure of both thermal plasma and the injected beam. Under the present experimental conditions, these configurations give a smaller helical ripple at the plasma center then other magnetic axis positions. When the magnetic axis is shifted outwards ($R_{ax} > 97$ cm), the toroidal rotation speed decreases below 10 km/s.

Electron temperature dependence on magnetic axis position

It has been observed that the electron temperature for co-injected NBI plasmas increases when the magnetic axis position is shifted inward to $R_{ax} = 92$ cm. In experiments with counter-injection the dependence of the electron temperatures on R_{ax} is quite different from the co-injected case. The electron temperature does not increase when the magnetic axis is shifted inward. A possible reason for it is as follows. In CHS, the inward-shifted configuration has the plasma boundary determined by the inner wall as a limiter. Though the injection is tangential, the beam ion orbits deviate from magnetic surfaces due to the toroidal drift effects. Since the deviation of orbits is inward for the counter-injection case, a significant part of beam ions hit the inner wall and are lost when the magnetic axis is shifted inward. It is expected that, for the counter-injection case, such effects cancel out the improvement of confinement with the inward shift of magnetic axis. Monte Carlo simulation results made by Dr. K. Hanatani of Kyoto University (HELIOS code) support this interpretation.

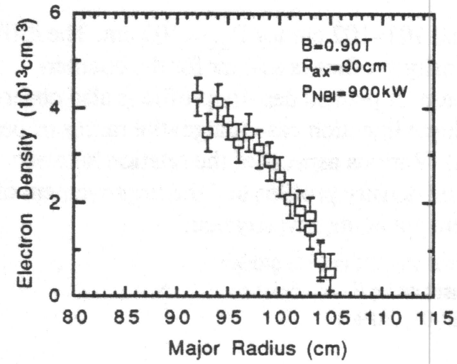

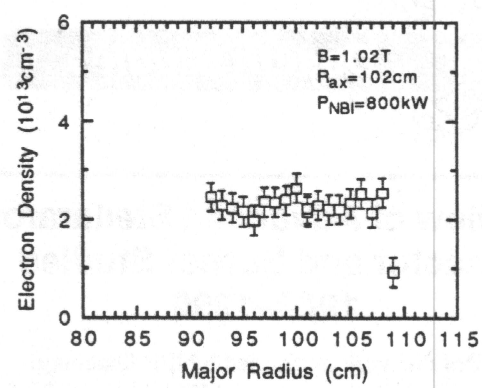

Density profiles in CHS for two different positions of the magnetic axis.

More peaked density profile of NBI plasma with inward magnetic axis shift

The density profiles of the NBI plasmas in CHS were very flat for most cases ($R_{ax} > 95$ cm). More peaked density profiles are observed when the magnetic axis is shifted inward. Two typical cases for co-injection NBI are shown for $R_{ax} = 102$ cm and 90 cm. The major radius of the ion temperature peak is 93–94 cm for R_{ax}

alous electron thermal conduction according to Lackner, the plasma parameters required for ignition were rather high: B = 6.5 T, n(0) = 3×10^{20} m^{-3}, average beta = 8%. If the anomalous thermal conductivity follows the Horton drift wave model, the confinement is higher by a factor of 2, leading to much lower ignition parameters: B = 5.5 T, n(0) = 1.65×10^{20} m^{-3}, average beta = 3.7%, fusion power = 2.6 GW. Corresponding average power loads at the first wall are around 1.5 MW/m^2. Higher power output could be achieved by increasing the density. These results show that ignition requires a reduction of L-mode transport similar to that needed in tokamak reactors. Reduced major radii of the reactor would lead to increased beta values.

Average beta values of 4.3–5.3%, as seen in calculations for B = 5.0 T and a major radius R ≈ 20 m at an aspect ratio of 12.5, are approximately consistent with the calculated stability limit of the Helias configuration chosen for Wendelstein VII-X . The corresponding fusion power values of the Helias reactor of approximately 2.8–4 GW are reasonable in view of present power stations.

A maintenance scheme similar to that studied in the ASRA6C report should be applicable for the Helias reactor. One of the options under discussion considers a system separated in half field periods for end-on maintenance and complies with the helical topology. Data obtained in the ASRA6C Study for the blanket and shield appear to be valid for Helias reactor and burner systems. The influence of the helical geometry on the breeding ratio needs to be quantified.

A more complete investigation of Helias reactor or burner systems is needed. It would be substantiated by experimental evidence expected from the present Advanced Stellarator Wendelstein VII-AS, and, in the future, from Wendelstein VII-X, in the fields of plasma transport, stability, and plasma edge physics, under the influence of configurational effects such as those of a magnetic separatrix, islands, or stochasticity.

ASR and ASB studies so far have been performed on the assumption of certain plasma properties, involving extrapolations or even speculations of the reactor performance. These were extremely helpful for the assessment of prospects, in order to point out critical issues.

Future work should go in the opposite direction, starting from requirements to reach the essential goals, (e.g., transport versus size, beta value versus magnetic field, properties of the exhaust system, and power handling). Results from, and projections for, complementary approaches should be compared and judged before aiming at a point study of the reactor performance at a later time.

[1] Böhme, G., et al., Reports IPP Garching 2/285 (1987), KfK Karlsruhe 4268 (1987), and University of Wisconsin FPA-87-2 (1987).

[2] Grieger, G., et al., Proc. 4th IAEA Conf. and Workshop on Fusion Reactor Design and Technol., Yalta, 1986, **1**, IAEA, Vienna (1987), 341.

[3] Hübner, J., and Maurer, W., Proc. 4th IAEA Conf. and Workshop on Fusion Reactor Design and Technol., Yalta, 1986, **1**, IAEA Vienna (1987), 333.

[4] Harmeyer, E. et al., Proc. 4th IAEA Conf. and Workshop on Fus. Reactor Design and Techn., Yalta 1986, **1**, IAEA, Vienna (1987), 361.

[5] Harmeyer, E., et al., Proc. 4th IAEA Conf. and Workshop on Fusion Reactor Design and Technol., Yalta, 1986, **1**, IAEA, Vienna (1987), 375.

[6] Maurer, M., Proc. 4th IAEA Conf. and Workshop on Fusion Reactor Design and Technol., Yalta, 1986, **1**, IAEA, Vienna (1987), 407.

[7] Harmeyer, E., et al., Proc. 4th IAEA Conf. and Workshop on Fusion Reactor Design and Technol., Yalta, 1986, **2**, IAEA, Vienna (1987), 37.

Fritz Rau
Max Planck Institut für Plasmaphysik
Association EURATOM-IPP
W-8046 Garching, FRG

stellarator news

Published by Fusion Energy Division, Oak Ridge National Laboratory
Building 9201-2; P.O. Box 2009; Oak Ridge, TN 37831-8071, USA

Editor: James A. Rome | Issue #13 | January, 1991

Eighth International Workshop on Stellarators

The Eighth International Workshop on Stellarators will be a Technical Committee Meeting of the International Atomic Energy Agency and will be hosted by the Kharkov Institute of Physics and Technology and the State Committee on Atomic Energy of the USSR. The workshop will be held May 27–31, 1991 in the conference hall of the Kharkov Institute of Physics and Technology.

The workshop will cover all topics applicable to stellarators and other helical confinement devices. Topics of interest are: experimental results, theory, diagnostics of special interest to helical devices, and future devices. The number of oral presentations will be limited to emphasize overview talks, reviews of recent works, and topics of general interest. More detailed papers will be presented in poster sessions. Ample time will be set aside for free discussion.

Participation in the Workshop is limited to 120 persons. Interested persons should notify the Workshop Secretary, Dr. V. Tereshin, of their intention to attend the meeting and provide a tentative title of their presentation (and whether poster or oral presentation is preferred) by January 31, 1991. A one-page abstract of each paper is needed by March 4, 1991.

V. Tereshin
Kharkov Institute of Physics and Technology
Plasma Physics Division
Academicheskaja, 1
Kharkov 310108, USSR
Telephone: (007)-(057)-2351993, ext. 015
FAX: (007)-(057)-2352664
Telex: 115 175 DECAN SU

Around the Labs

Record high-speed pellet injector

A two-stage pneumatic pellet injector for Heliotron E, with relevance for other magnetic confinement machines, has been constructed and tested in order to provide increased pellet velocity. The increased velocity will allow more flexible control of the density profile of the Heliotron E plasma and will produce a wider range of pellet velocity for pellet ablation studies. Pellet velocity is limited to around 1.4 km/s for the present six-pellet injector on Heliotron E, which has successfully operated for several years.

The fundamental operation of the new pellet injector was simulated using the code Quickgun developed by Dr. S. Milora of ORNL. The experimental results generally agree well with the code calculations if we assume an effective diameter for the fast valve orifice. By devel-

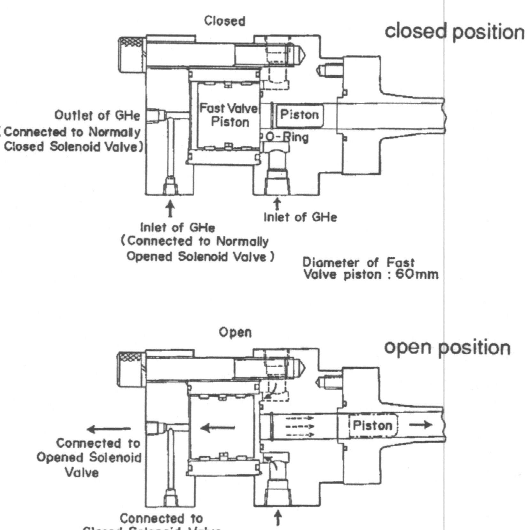

Schematic of the high-pressure fast valve

Oak Ridge National Laboratory is managed by Martin Marietta Energy Systems, Inc. for the U.S. Department of Energy

oping a high-pressure fast valve, we have achieved a hydrogen pellet velocity of 3.2 km/s without using a sabot. This is the world record for hydrogen pellets without sabots.

The high performance of this two-stage injector is partly due to a specially developed high-pressure fast valve with a very large conductance as shown in the figure. We studied the dependence of the pellet velocity and breech pressure on the pump tube fill pressure. The results show that the fill pressure is a very sensitive parameter. We also investigated the effect of the clearance between piston and pump tube wall on the pellet velocity, and the exhaustion and damage of the piston caused by the compressing propellant gas. The changes to the piston surface differ quite a lot depending on whether the fill gas is hydrogen or helium.

Shigeru Sudo
Plasma Physics Laboratory
Kyoto University
Uji, Kyoto, Japan

News from CHS

Experimental study of the field error effects on confinement has been carried out under the US/Japan collaboration program. Two error field coils mounted on the top of the CHS device with 180° separation between them in the toroidal direction can produce a vertical error field of the order of 10 G at the plasma center in the experiment with a 1-T magnetic field. Islands of $m = 2$, $n = 1$ are produced at the $q = 2$ surface, when the current directions for the two coils are opposite.

Experiments were carried out both for ECH and NBI plasmas at a magnetic axis of $R_{ax} = 100.8$ cm (outward shifted). This configuration was chosen so that the width of the $m = 2$ island becomes large, because the magnetic shear at the $q = 2$ surface is small. The stored energy measured by the diamagnetic loop was reduced by 10–20% for the NBI plasma with the perturbation coils excited. The difference in the diamagnetic loop signal is more significant for the ECH case though the noise due to magnetic field ripple is larger. The radial profiles of the electron density and temperature have been measured by Thomson scattering. The toroidal phase of the island (O-point or X-point) at the Thomson scattering chord can be changed by reversing the current direction. No clear difference between ECH and NBI plasmas was observed with the profile measurement, although we have only preliminary data. The disagreement of the two diagnostics is not yet understood. Vacuum magnetic surface mapping with the error field is planned.

A lithium pellet injector is now operational and initial testing has been carried out. Increases in line density and stored energy with an appropriately sized pellet were observed without radiation collapse. This is different from the previous hydrocarbon pellet injection experiment. The experiment will continue in January.

Special diagnostic systems have been set up for neutral hydrogen measurements. The poloidal and toroidal arrays for the H_α emission detector system are now absolutely calibrated. A laser fluorescence method is to be applied soon. Those diagnostics have progressed under a collaboration with Kyushu University. Improved understanding of particle transport is a goal of the experiment.

Harukazu Iguchi for the CHS Group
National Institute for Fusion Science
Nagoya, 464-01 Japan

Development of Kyoto negative ion source

During the past several years, the Heliotron-E NBI system has revealed a number of interesting physics issues that should be explored to find the best confinement regimes in helical systems. One recent exciting topic was concerned with magnetic configuration studies, by which a new regime of improved confinement was found using additional toroidal and vertical fields. Data analysis of these MHD/transport results is now under way.

The NBI group is now developing a next-generation NBI system which uses negative ion sources in a high-energy regime [1]. The ion source is a modified version of a circular cylindrical bucket-type positive ion source (30 cm diameter, 19 cm long), in which a magnetic filter of the rod type is housed. The filter divides the arc chamber into two regions: (I) driver volume and (II) extraction volume.

To understand the underlying atomic and molecular processes that occur in the Kyoto negative-ion source, measurements of plasma parameters were made using electrostatic probes, spectral emission lines, and a photodetachment technique.

The novel photodetachment technique was applied to measure the H^- density (n_-) in chamber II. The Nd-YAG laser (1.064 μm) of 8-mm diameter, 30-ns duration, and 30-mJ energy was used to detect the photodetachment electrons emitted from the laser-illu-

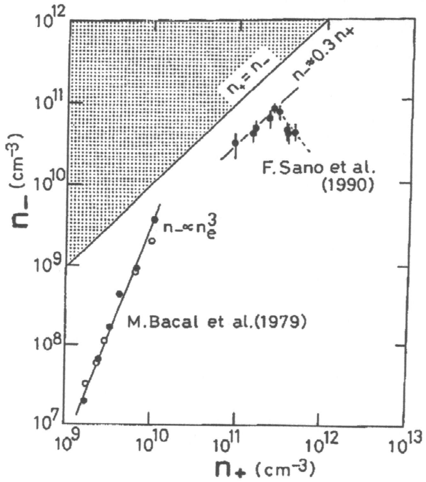

Fig. 1. H^- ion density (n_-) as a function of positive ion density (n_+). Our data are compared with Bacal's data which shows a marked difference of H^- confinement behavior.

minated region. The present laser energy is at a sufficient level for achieving the $\Delta n_-/n_-$ saturation requirement. Photodetachment signals with a different material gases (H_2, He and D_2) were compared in order to confirm the photodetachment mechanism occurring in the detection region. H^- density characteristics in chamber II, as determined by this technique, so far satisfactorily explain the behavior of the extracted negative ion current density on the beam axis. The H^- density behavior obtained here has been compared with that of the pioneering work by M. Bacal et al. [2] as shown in Fig. 1. Although Bacal's data show the relation of $n_- \propto n_e^3$, our data indicate $n_- \approx 0.3 n_+$ (or $n_- \approx 0.42 n_e$) under optimal conditions in the much higher density region.

The observed behavior clearly shows that the loss of negative ions is dominated by destruction (mutual neutralization and detachment in electron collisions) rather than by diffusion. Equilibrium rate calculations including the dominant effects of vibrationally excited hydrogen molecules ($H_2(v'' = 7\sim 10)$) also support this interpretation. This experimental result predicts $H_2(v'')$ wall bounces on the order of 10 to 40 if the wall-related $H_2(v'')$ reaction rates are small. The comparison with theory (provided by J. R. Hiskes et al. [3]) is interesting and should be done, in combination with the experimental data of $H_2(v'')$ distribution. A model predicts that the $H_2(v'')$ density $n(v'') \approx 8.4 n_+$ for our experimental conditions.

In order to estimate the H^- emission current density, the experimental determination of the H^- ion thermal velocity $\langle v_- \rangle$ in chamber II is very important. An approach to estimating $\langle v_- \rangle$ is to analyze the plasma dynamics subsequent to photodetachment. The time at which the probe current returns to zero, Δt, was assumed to correspond to the arrival of a group of slow H^- ions. Therefore, $(v_-)_{min} = (R - r)/\Delta t$, where R is the radius of the laser beam and r is the radius of the probe. A typical value of $\Delta t \sim 0.5$ µs, as shown in Fig. 2, provides $(v_-)_{min} \sim 2$ km/s, which is over a factor of 2 smaller than the theoretical $(v_-)_{min} \sim 5.2$ km/s predicted by J. M. Wadehara [4].

The characteristics of n_-/n_e as a function of arc current showed that the ratio n_-/n_e increased with an increase in source pressure at high arc currents. However, with D_2 operation n_-/n_e was a factor 3 ~ 4 lower than with H_2 operation. The reason is not yet clear, and now related studies are under way.

Application of a positive bias voltage between the arc chamber and the plasma grid enhanced the ratio of n_-/n_e up to ≈ 1, which means that half of the negative charges in chamber II were ascribed to H^- (!).

With the progress of grid conditioning, a factor OF 2 increase in acceleration voltage (13–27 kV) recently resulted in a remarkable increase of the extracted H^0 + H^- current density (calorimeter detected $H^0 + H^-$ current/9-hole area). At present, an arc current of more than 400 A at 27 kV can provide a current density of >20 mA/cm^2.

[1] F. Sano et al., US-Japan Workshop on Negative Ion Based NBI Development, Berkeley, CA, Oct. 8–11, 1990.

[2] M. Bacal and G. W. Hamilton, Phys. Rev. Lett. **42** (1979) 1583.

[3] J. R. Hiskes and A. M. Karo, Appl. Phys. Lett. **54** (1989) 508.

[4] J. M. Wadehara, Phys. Rev. A **29** (1984) 106.

Fumimichi Sano
Plasma Physics Laboratory
Kyoto University
JAPAN

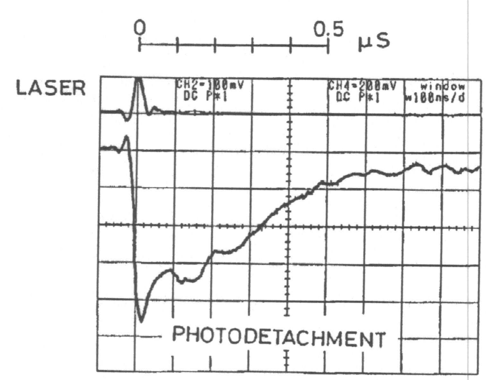

Fig. 2. Time evolution of the photodetachment signal in chamber II. A typical dacay time is on the order of 0.5 µs.

News from ATF

While the ATF is shut down for a transformer upgrade, data obtained during the last operation period have been analyzed. Transport and fluctuation data in the quadrupole field scan with neutral beam injection are of particular interest. In this scan, the quadrupole field was varied in the same way as in the bootstrap current studies with the vacuum magnetic axis $R_0^{(vac)}$ fixed at 2.08 m (with $\bar{n}_e = 5.3 \times 10^{19} \text{m}^{-3}$ and $P_{NBI} = 0.8$ MW). Figure 1(a) shows variations of the central and volume-average beta, β(0) and ⟨β⟩, calculated from the profile analysis. The lengths of the bars representing β(0) indicate fast-ion contributions to β(0). The global energy confinement time $\tau_E^* = W_{dia}/P_{abs}$) based on the estimated absorbed power P_{abs} is equal to the kinetic gross energy confinement time, $\tau_E(a) = (W_e + W_i)/(P_{be} + P_{bi})$, based on calculated beam power transfer to electrons (P_{be}) and ions (P_{bi}) from the profile analysis. The energy confinement times peak in the vicinity of the standard or slightly prolate configurations, as in the quadrupole scan with ECH alone. This trend is consistent with that of the thermal electron diffusivity derived from a local power balance [Fig. 1(c)]. The pressure profile shape is also affected by the quadrupole field variations. Figure 1(b) shows the ratio β(0)/⟨β⟩ as a function of the quadrupole field. The pressure profiles become more peaked as the flux surfaces become more oblate. In spite of modest beta values with modest NBI power, the Shafranov shift is rather large ($\Delta_S/\bar{a}$ up to 0.25) for the oblate configuration. These variations of the pressure profiles and Shafranov shifts have significant effects on stability and fluctuations.

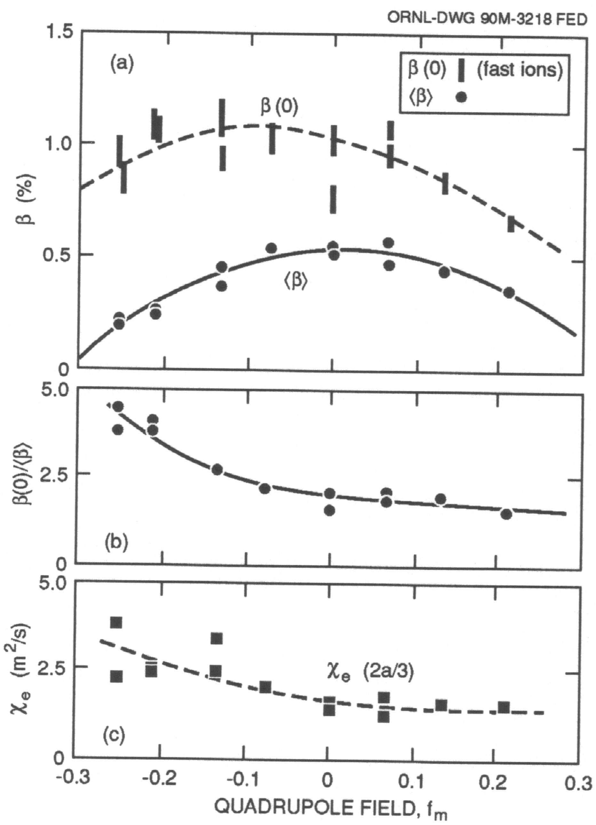

FIG. 1. Response of plasma parameters to the quadrupole field scan with NBI (R_0^{vac} = 2.08 m and B_0 = 0.95 T): (a) central and volume-average beta, (b) ratio of central to volume-average beta, and (c) electron thermal diffusivity at r = 2a/3, as a function of the quadrupole field ratio.

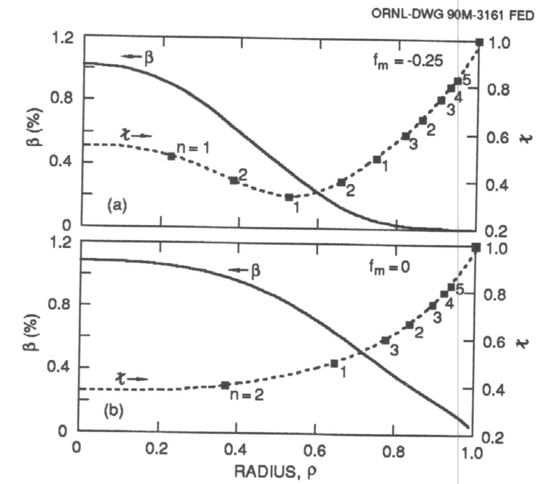

Fig. 2. Radial profiles of beta and rotational transform and resonance toroidal mode numbers for two cases in the NBI quadrupole scan: (a) narrow pressure profile case with f_m = 0.25 and (b) peaked pressure profile case with f_m = 0.

Figure 2(a) shows the effects of narrow pressure profiles on magnetic fluctuations with the quadrupole field ratio $f_m = -0.25$. The pressure profile is reminiscent of the profiles observed before the field error repair (but not as peaked). Double resonances at ɩ = 1/2, 2/5, and 1/3 appear in the middle radial region ($0.2 < \rho < 0.8$) where the pressure gradient is at a maximum. The magnetic fluctuations observed with Mirnov coils show globally coherent modes with low toroidal mode numbers, n = 1 and 2. However, the central beta in these experiments was too low to reach the critical value above which the self-stabilization (second stability) dominates.

Effects of broad pressure profiles are represented by the $f_m = 0$ case [Fig. 2(b)] in the NBI quadrupole scan. The broad pressure profile is typical of profiles obtained after the field error repair. There is no double resonance in $\iota\!\!-(\rho)$, and the maximum pressure gradient appears near the plasma edge, where the resonances have higher n numbers. The observed fluctuations have higher n (n = 1–6) with short toroidal coherence lengths ($\Delta\varphi \approx$ one field period = 30°) Detailed studies of the harmonic spectra of $\tilde{B}$ signals in the operation period show that the rms fluctuation level of the coherent $\tilde{B}$ increases with increasing $\langle\beta\rangle$. At high beta, the $\tilde{B}$ signals are dominated by more toroidally localized disturbances at the edge of the plasma, where the local magnetic field curvature in the helical ripple wells is strongly destabilizing.

With the present broad pressure profiles, the beta values are still too low to show self-stabilization. Access to the second stability regime requires higher beta (with higher beam power) and/or more peaked profiles. A pressure profile control experiment with dynamic configuration variations using the quadrupole field would be an attractive way to access second stability in full bore ATF plasmas.

M. Murakami and J. H. Harris for the ATF Group
Oak Ridge National Laboratory
P.O. Box 2009
Oak Ridge, TN 37831-8072, USA

People

Visitors to the CHS Group

Dr. Larry Peranich (General Atomics, USA) stayed for seven weeks in October to participate in the experimental study of the effect of the error field on the confinement, which is discussed in "News from CHS" above.

Dr. Shinji Hiroe (Oak Ridge National Laboratory, USA) visited CHS in November and discussed radiation losses in ECH and NBI plasmas.

Design Studies

Determination of LHD Machine Configuration

Design Work History

The Large Helical Device (LHD) project is a major fusion research program under the Ministry of Education, Science and Culture. In 1986, the Nuclear Fusion Subcommittee of the Science Council recommended that a large helical device should be build in Toki City, Gifu Prefecture. Responding to this recommendation, the LHD design group was organized. In fiscal year (FY)1986, the LHD objectives were clarified and the l = 2 Heliotron/Torsatron-type continuous-coil configuration was adopted (see the Green LHD Design Book). Superconducting coil systems with m (helical pitch number) of 10–14 were studied in FY 1987 (see the Blue Design Book), and the standard magnetic configurations was selected as m = 10, γ (helical pitch parameter) ~1.2 in FY 1988 (see the Orange Design Book). After the foundation of the National Institute for Fusion Science (May 29,1989), a final machine configuration was chosen under the LHD Design Group.

Choice of Magnetic Configuration

Through several-years of design work, the optimal value of m was found to be near 10 for the LHD system with respect to compatibility among several physics and engineering requirements. The final magnetic configuration for LHD has been mainly determined by the following physics requirements within the related engineering constraints;

- High beta achievement ($\beta \geq 5\%$).
- Good confinement of energetic particles (loss-cone-free radius ($r_L \geq a_p/3$) for 70% ICRF heating efficiency).
- Divertor-wall clearance ($\Delta_{dw} \geq$ 3 cm).
- Maximization of transport properties.

The beta limit and the divertor condition require the m ≤10 for a medium-γ_c configuration ($\gamma_c = ma_c/lR \sim$ 1.2–1.3). A higher-γ_c configuration ($\gamma_c \geq 1.3$) cannot provide the divertor-wall clearance for 4-m/4-T LHD designs with an allowable coil current density of ~ 50 A/mm^2. In LHD a slight positive pitch modulation of the helical windings ($a_c = 0.1$, $\theta = (l/m)\ \varphi + a_c \sin(l\ \varphi/m)$) is found to improve physics-engineering compatibility. A negative pitch modulation improves orbit confinement for small inward axis shift; however, the positive pitch modulation leads to more improvement for large inward shift.

As design candidates, we chose three systems,

(A) $m=10$, $\gamma_c=1.20$, $a_c=0.0$,
(B) $m=10$, $\gamma_c=1.20$, $a_c=0.1$,
(C) $m=10$, $\gamma_c=1.25$, $a_c=0.1$,

and compared their magnetic confinement properties of these three designs as a function of inward shift Δ_{ax}. For the (B) design, the compatibility between beta and orbit criteria is not satisfied. In the (A) and (C) designs, three conditions are matched at $\Delta_{ax} \sim -12.5$ cm and $\Delta_{ax} \sim -15$ cm, respectively.

Table 1. Specifications of LHD

Parameter	Phase I	Phase II
l	2	2
m	10	10
γ_c (pitch parameter)	1.25	1.25
a_c (pitch modulation)	0.1	0.1
Major Radius	3.9 m	3.3 m
Plasma Minor Radius	0.6–0.65 m	0.6–0.65 m
Plasma Volume	30 m^3	30 m^3
Magnetic Field	3.0 T	4.0 T
Helical Coil		
Magnetomotive Force	5.85 MAT	7.80 MAT
Current Density	40 A/mm^2	53.3A/mm^2
Coil Temperature	4.2 K	1.8 K
Maximum Field	7.2 T	9.6 T
Poloidal Coil		
Outer Vertical	-4.3 MAT	-4.3 MAT
Inner Shaping	-4.4 MAT	-4.4 MAT
Inner Vertical	4.9 MAT	4.9 MAT
Divertor		
Baffle Plate		Installed
Plasma duration	10 s	10 s
Repetition time	5 min	5 min
Heating		
ECH	10 MW	10 MW
NBI	15 MW	20 MW
ICRF	3 MW	9 MW
Steady-State Power		3 MW

In addition to these three conditions, we checked the neoclassical and anomalous transport rates. Among the three design options the maximum $n\tau T$ value can be obtained in the (C) design. Moreover, the (C) configuration is better than (A) from the viewpoint of reducing poloidal coil currents.

The final magnetic configuration for LHD was determined to be the optimized configuration ($l=2$, $m=10$, $\gamma_c=1.25$, $a_c=0.1$).

Engineering Design and R&D Programs of LHD

The machine design was carried out to satisfy the above mentioned design configuration, and the final specification of the LHD system have been determined as shown in Table 1. The experimental program is divided into two phases. To promote the LHD construction, several research and development (R&D) programs are being carried out.

Schedule of LHD Project

The budget for the first year of the seven-year construction period was approved by the Japanese government in 1989. The construction of LHD will be completed in 1997.

LHD Design Group
National Institute for Fusion Science
Nagoya 464-01, Japan

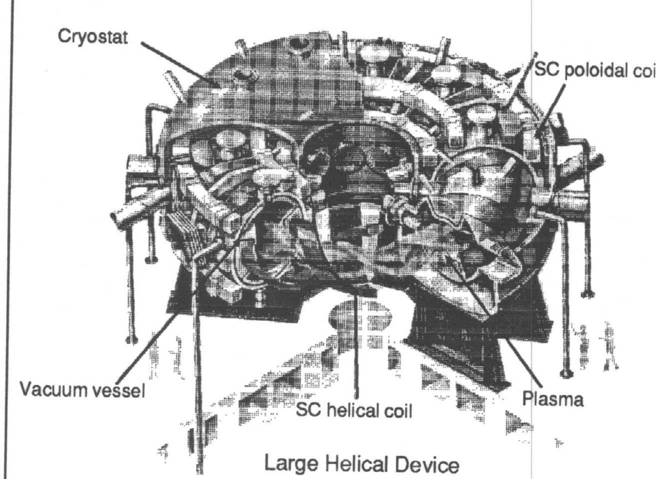

Large Helical Device